Evaluation of Energy Transfer Efficiency and Path-Tracking Performance for an Autonomous Truck Model with Dynamic Wireless Charging

Mats Jørgensen[1)], Giuseppe Guidi[2)], Jon Are Suul [1),2)]

1) Department of engineering cybernetics, Norwegian University of Science and Technology, Trondheim, Norway

E-mail: jon.are.suul@ntnu.no

2) SINTEF Energy Research, Trondheim, Norway

E-mail: Giuseppe.Guidi@sintef.no

ABSTRACT: This paper presents the results from experimental testing of a dynamic wireless charging system for an autonomous truck model in scale 1:14. The truck model is equipped with functionality for autonomous operation by computer-vision-based path tracking and tested on a track that includes a charging section with two coils for dynamic wireless inductive power transfer (DWPT). A path tracking algorithm based on two cameras is shown to provide consistent lateral positioning along the track, which ensures that the truck is approximately centered with respect to the road-side coils when passing the charging section. The road-side coils are automatically activated from the truck when approaching the charging section, and the dc power input to the road-side converters as well as the power output to the on-board battery are logged during the charging cycles. The impact of activating the road-side coils at different positions of the truck is evaluated with respect to the power transfer profile and the overall energy transfer efficiency. It is discussed how the energy transfer efficiency can be increased by transferring power only when the entire vehicle-side coil is above the road-side coil. It is also shown how unnecessary losses will be caused by activating the power transfer before reaching the point when half of the vehicle-side coil is above the road-side coil, corresponding to the point of zero magnetic coupling. However, the total energy transferred to the on-board battery can be maximized by activating the road-side coils close to the point of zero magnetic coupling, and it is demonstrated that this is achieved without causing any significant reduction in the energy transfer efficiency.

KEY WORDS: Autonomous Vehicles, Camera Vision, Dynamic Wireless Charging, Electric Vehicles, Energy Transfer efficiency, Inductive Power Transfer, Path-Tracking.

1. INTRODUCTION

Several concepts for wireless inductive power transfer to moving vehicles have been developed during the last decade, as reviewed in [(1),(2)]. Thus, several demonstration projects have also been initiated during the last years to verify the practical operation of on-road dynamic wireless power transfer (DWTPT) technology for powering electric vehicles. In Europe, two separate demonstration sites have been developed in the European Union-funded project "FABRIC"[(3)], and a large-scale test-arena has been opened in Italy during 2021. At the same time, the SmartRoad Gotland project in Sweden is providing the first experiences with operation of wireless charging technology on a public road[(5)].

In parallel with the development of DWPT concepts, significant progress has been made towards achieving self-driving technology with practical applicability for road vehicles[(6)]. Thus, gradual emergence of autonomous vehicles for various purposes is expected over the coming decade. When considering the anticipated development of self-driving technology in the context of the increasing utilization of electric vehicles (EVs) for reducing emissions from road transport, the combination with contactless inductive charging technology can provide several appealing advantages[(7)]. Indeed, the combination of automated inductive charging and self-driving technology can enable fully autonomous operation of EVs with self-sufficient energy supply managed by the vehicle itself without the need for manual intervention[(8)]. This opportunity could be provided by both static and dynamic charging systems, but the possibility for dynamic on-road power transfer could enable significantly better utilization of the vehicles and their battery capacity.

While the potential advantages of DWPT technology applied to autonomous vehicles are easily identifiable, the installation cost of the infrastructure is expected to be one of the main challenges for deployment of the technology. Furthermore, it should be expected that the technology will only be installed in selected sections of a

road distance. Thus, it will be important to maximize the utilization of the infrastructure for energy transfer to each vehicle.

This paper presents an example of how DWPT technology can be utilized by autonomous vehicles and discusses how the strategy for activating the DWPT system influences the total energy transfer capability and the energy transfer efficiency. For this purpose, a miniature model of an autonomous truck in scale 1:14 with a correspondingly designed DWPT system is utilized. Path tracking functionality is implemented on the autonomous truck model and utilized to provide an autonomous vehicle operation as a basis for evaluating the energy transfer when the vehicle is passing over a set of road-side coil sections. The obtained results demonstrate how different strategies for activating the road-side coils influences the total energy transferred to the vehicle and the corresponding energy transfer efficiency. Thus, it is discussed how the energy transfer to the vehicle can be maximized by keeping the road-side coil in operation during the transients when the vehicle is entering and leaving the available area for power transfer. By limiting the time of power transfer to the period when there is a high coupling between the road-side coil and the receiving coil, the energy transfer efficiency can be slightly improved but at the cost of reduced total energy transfer. It is also demonstrated that activation and deactivation close to the point of zero magnetic coupling when entering and leaving a road-side coil section can ensure close to maximum total energy transfer without causing any significant reduction of energy transfer efficiency.

2. SYSTEM DESCRIPTION

The system configuration used for the presented experiments is based on a commercially available radio-controlled electric truck model in scale 1:14. This truck model has been modified by introducing an inductive charging system and a platform for autonomous operation. In addition, the studied configuration includes two road-side coil sections design for dynamic inductive power transfer to the vehicle. A picture of the small-scale autonomous truck model while in operation is shown in Fig. 1. The details of the DWPT system and the platform for autonomous operation of the vehicle are presented in the following.

2.1. Inductive power transfer system

The applied DWPT system has been designed to equivalently represent a 200 kW system for a regular truck, as further described in [8],[9]. Thus, the geometrical dimensions of the on-board coil are also assumed to be in the scale of 1:14. A picture with a closer view of the on-board coil is also shown in Fig. 1. The considered DWPT system includes two road-side coils, which are designed

Fig. 1. Picture of 1:14 scale autonomous truck model with camera-based path tracking functionality when passing a road-side coil section for DWPT, with a closer view of the on-board coil shown in the lower left side the figure.

Table 1 Parameters of Small-scale test system

Nominal power, P_0	75 W
I/O voltages, $V_{dc,in}$ $V_{dc,out}$	12.0 V, 7.4 V
Nominal operating frequency, f_n	75 kHz
Vehicle-side coil	
Planar dimensions	100 x100 mm
Self-inductance (above road-side coil), L_2,	7.9 μH
Resonance frequency (above road-side coil)	78 kHz
Quality factor Q_2, (at 75 kHz)	163
Road-side coil 1	
Planar dimensions	570 x100 mm
Self-inductance (with no pick-up), $L_{1,1}$	36.7 μH
Resonance frequency (with no pick-up)	74 kHz
Quality factor $Q_{1,1}$ (at 75 kHz)	293
Road-side coil 2	
Planar dimensions	440 x 100 mm
Self-inductance (with no pick-up), $L_{1,2}$	31.0 μH
Resonance frequency (with no pick-up)	74 kHz
Quality factor $Q_{1,2}$ (at 75 kHz)	143
Coupling conditions	
Airgap distance	22 mm
Coupling factor, k (centered, max coupling)	0.16, 0.18

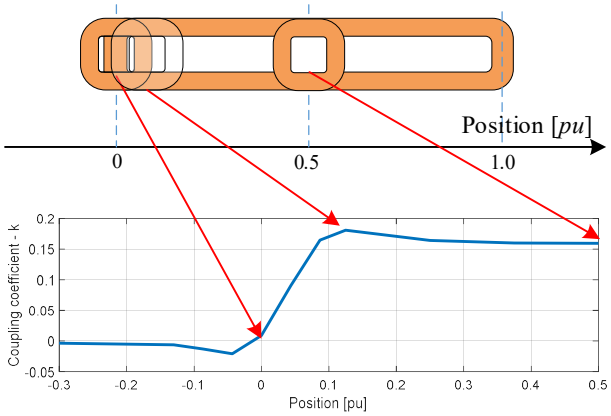

Fig. 2. Coupling coefficient as function of on-board coil position

with different lengths and different parameters to assess the impact on the energy transfer capability. All the coils of the DWPT system have series capacitor compensation and the resulting main parameters of the system are listed in Table 1. Fig. 2 shows the

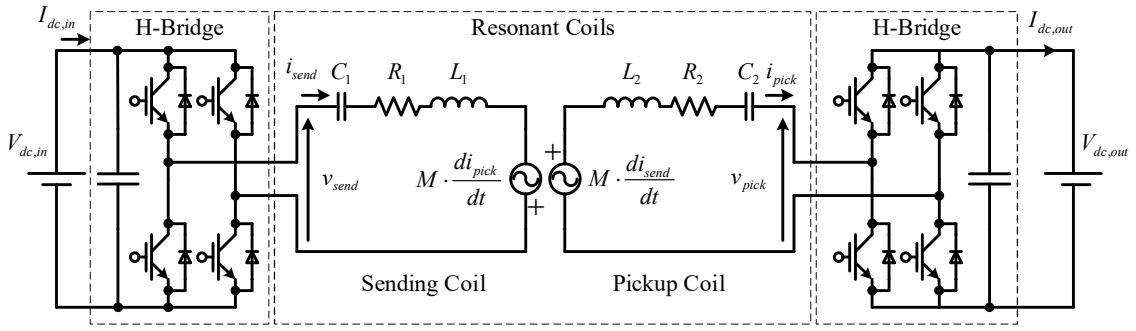

Fig. 3. Applied topology of SS-compensated DWPT system with H-bridge converters on both sides.

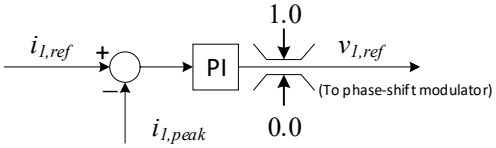

Fig. 4. Current control of road-side coil

magnetic coupling coefficient *k* between the road-side coil 1 and the on-board coil as a function of the position when the truck is passing over the charging section. As seen in the figure, the coupling coefficient has a small negative value before reaching the point with zero magnetic coupling. When more than half the on-board coil is above the road-side coil, the coupling coefficient is increasing quickly, and reaches a peak of about 0.18 before settling at a value close to 0.16 when the on-board coil is above the middle of the road-side coil.

Identical H-bridge converters are utilized for controlling both the road-side coils and the on-board coil. This results in the circuit diagram of a conventional series-series (SS)-compensated inductive charging system with an active receiving side converter, as shown in Fig. 3. However, the on-board H-bridge converter is controlled for synchronous rectification, and thereby operates as a diode rectifier with the battery appearing as a constant voltage load (CVL) as seen from the sending side converter.

As seen from the parameters in Table 1, the on-board and road-side resonant coils are designed with slightly different resonance frequencies. This de-tuning is introduced to achieve slightly inductive characteristics as seen from the sending coil, which ensures zero voltage switching of the sending-side H-bridge[10],[11].

When operating the on-board converter with synchronous rectification, the road-side converter will be responsible for the power control of the DWPT system. However, when the coupling between the on-board and road-side coils is low, the main function of the control for the sending side H-bridge converter will be to limit the current. Thus, a Proportional-Integral (PI) controller for the road-side coil current is used to provide the voltage reference for phase-shift modulation of the H-bridge converter, as illustrated in Fig. 4. If the desired power can be transferred without reaching the maximum sending side current or the maximum sending side voltage, the current reference can be provided by an outer loop power controller, as discussed in [12]. However, in this case, the power transfer in the operating regions with high coupling between the coils is limited by the available voltages for the road-side and/or receiving side converters, as discussed in [8]-[10].

2.2. Autonomous operation of the truck model

The radio-controlled truck model has been enhanced by introducing a platform for autonomous operation based on a Nvidia Jetson TX2 embedded computer. While several strategies for autonomous operation have been tested with this platform [13],[14], a computer-vision-based path tracking algorithm based on two cameras is the basis for the evaluation of autonomous operation with a DWPT system presented in this paper. For this purpose, the truck model has been operated on a marked lane running in a loop that included the DWPT section.

In the studied configuration, the system utilized two cameras to detect an area spanning 0-100 cm in front of the truck model. As seen from Fig. 1, one camera is mounted inside the cabin of the truck model, while the other is mounted on a tripod connected to the roof. The images captured by the two cameras were merged into a unified image at a frame rate of 30 frames per second, resulting in a final image of 640x940p [15]. The path lanes were filtered, and 10 center-points were identified in an evenly distributed manner across the image for the purpose of path tracking. An Ackermann steering model was utilized to calculate the steering angle for the truck model, by analyzing the different combinations of the center-points found from the image manipulation process[15].

To improve the steering performance of the truck model, a closed-loop control was introduced in the reference signal for the original servo controller. For this purpose, a feedback loop was soldered from the rotary potentiometer inside the original servo drive as described in[15]. A discrete-time PI controller was then utilized to track the setpoint obtained from the Ackermann steering

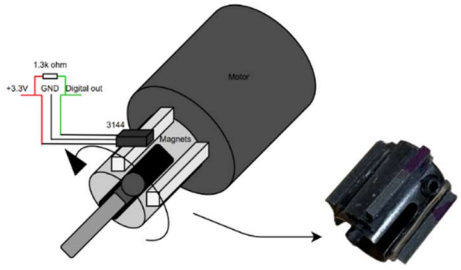

Fig. 5. Illustration of Hall-sensor-based position detector utilized to provide a speed measurement for closed loop control

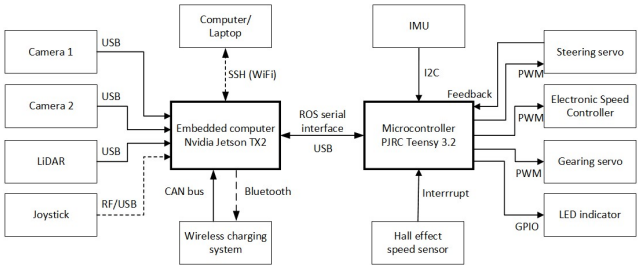

Fig. 6. Overview of hardware elements and interconnections for the autonomous truck model

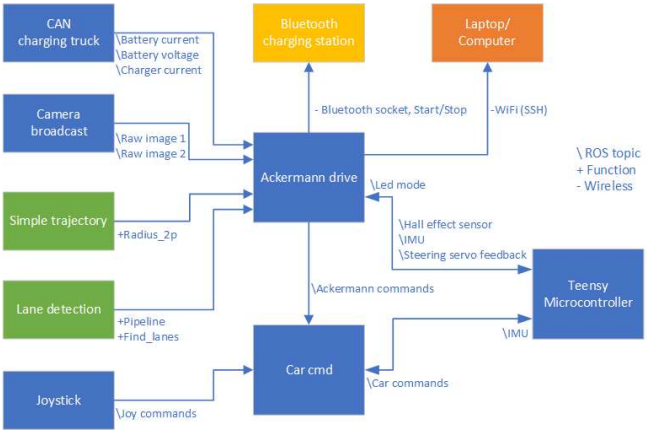

Fig. 7. Overview of software structure implemented on the Nvidia platform and the interfaces to the other parts of the system

model by utilizing the feedback provided by the rotary potentiometer.

To ensure a consistent and regulated speed of the truck model when passing over the DWPT section of the track, a closed loop speed control was also introduced. However, the truck model did not originally provide any accessible feedback signal for the driving speed. Thus, a Hall-effect sensor was utilized to detect the position of four magnet installed on the connection between the motor and the drive shaft, as illustrated in Fig. 5. One rotation of the motor corresponds to 10 cm driven by the truck model, and the four magnets gave a reading for every 2.5 cm of driving distance. The speed was calculated as the filtered derivative of the signal from the Hall-sensor and used as the feedback signal of a PI-controller for regulating the speed of the truck model.

An overview of hardware elements included in the model and their interconnections is shown in Fig. 6, while the general

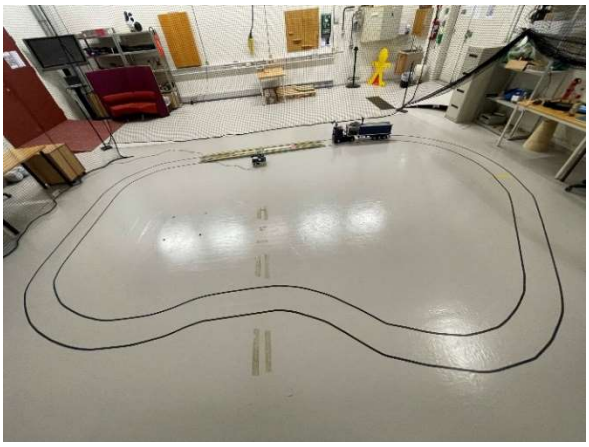

Fig. 8. Photo of the truck operating on the marked test track with the DWPT system

structure of the software implemented on the Nvidia Jetson TX2 embedded computer is presented in Fig. 7. The Nvidia platform is equipped with wireless connectivity capabilities, including built-in Wi-Fi and Bluetooth, with facilitate communication with a hand-held joystick used for operating the system, a computer for monitoring, and the stationary charging station. A CAN-bus connection was utilized for communication between the Nvidia unit and the control system for the on-board converter serving as an interface between the inductive charging coil and the battery. A LiDAR sensor was connected to the system via a serial interface and was primarily employed for mapping purposes. Finally, A Teensy microcontroller was installed within the truck model, to interface with the electronic components such as the Hall-effect sensor, the steering servo drive, the electronic speed controller of the truck model, and an inertial measurement unit (IMU). Further details on the utilized platform for self-driving functionality are documented in [13], while details on the implementation of the camera-vision based path tracking strategy are presented in [14],[15].

3. ASSESSMENT OF DWPT ENERGY TRANSFER EFFICIENCY DURING AUTONOMOUS OPERATION

To assess the autonomous operation with the DWPT system, the path tracking functionality is first verified for the track including the road-side coils. Then, the total energy transfer and the energy transfer efficiency that can be achieved by the DWPT system is evaluated with different strategies for activating the road-side coils.

3.1. Assessment of path tracking performance

The experimental setup for assessing path tracking performance and energy transfer efficiency involved a marked lane arranged in a loop, as shown in Fig. 8. For assessing the path tracking performance, the tuning of the PI controller for both speed and steering was first assessed and manually adjusted by imposing

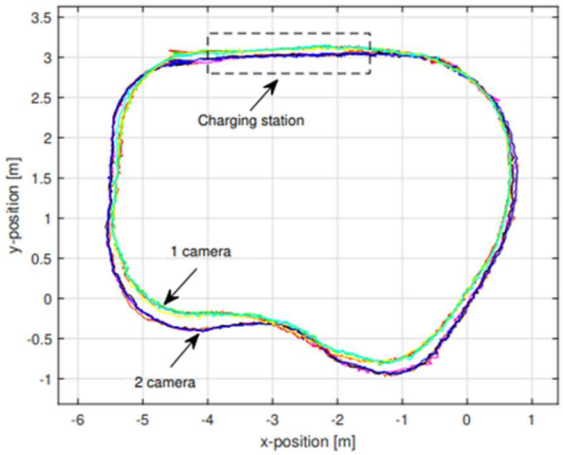

Fig. 9. Path tracking performance with one or two cameras, with position logged by LiDAR

step changes in the references, as further described in [15]. The performance was then evaluated when using one camera versus two cameras, by conducting four consecutive runs on the track for each condition. The position of the truck model was mapped using the LiDAR sensor, and the results are presented in Fig. 9, where curves in red, green, yellow, and cyan denote the use of one camera, while magenta, orange, blue, and black represented the use of two cameras. The charging station is marked on the figure in its approximate position and scale. The figure demonstrates a clear trend for each condition, exhibiting consistent path tracking performance with only minor deviations between each lap on the track. However, the control based on only one camera is less capable of following the curves of the marked track. Thus, the lateral positioning on the charging track is less accurate than with two cameras. As the case with two cameras provided more accurate tracking around sharp corners and while passing the charging section this case was used for further evaluation of the energy transfer from the DWPT coils.

3.2. Assessment of path tracking performance

As a starting point for evaluating the energy transfer efficiency, the operating conditions indicated in Fig. 10 are considered. The figure illustrates when the charging section defined by the road-side coil of the DWPT system is detected by the vehicle as well as when the null-points of the coupling between the road-side coil and the on-board coil zero occur. For all the following results, the truck is operated with the closed loop speed control having a reference of 0.4 m/s, which would correspond to a speed of approximately 20 km/h for a full-scale truck.

A first set of results, obtained when the road-side coils are activated 10 cm before the vehicle reaches the null-point of the coupling, is shown in Fig. 11. The curves in this figure clearly show how the activation of the road-side coil before the vehicle

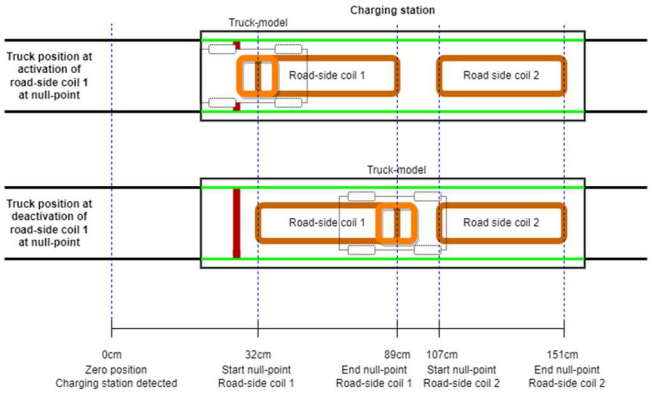

Fig. 10. Illustration truck position for an ideal sequence of activation and deactivation of the road-side coil

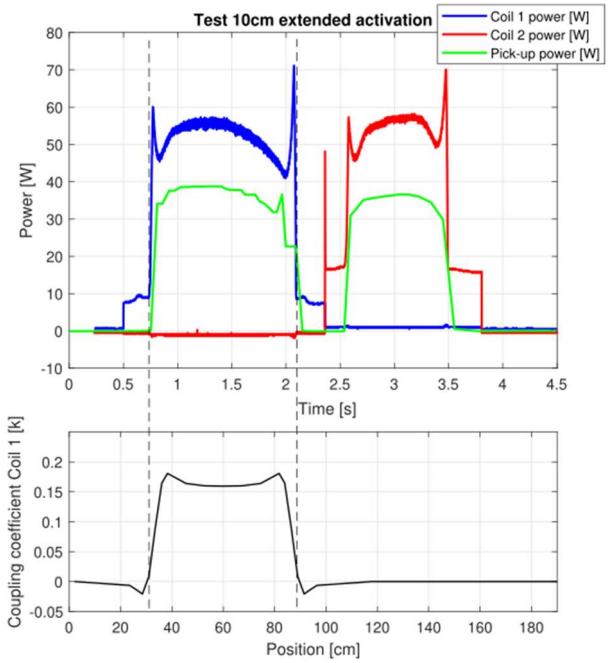

Fig. 11. Results for power transfer obtained when the truck-model is passing the road-side coils.

has passed the null-point of the coupling causes power losses on the sending side during a short period when there is no power transferred to the vehicle. Then, as soon as the vehicle passes the null-point of the coupling, as shown by the plot of the coupling coefficient in the lower part of the figure, a transient occurs as the system starts transferring power. By considering the ratio between the power supplied to the road-side coil and the power received by the pick-up coil on board the truck model, it can be understood that the losses are also relatively high during this transient response when the coupling between the coils is increasing rapidly. A similar transient response also appears when the vehicle is leaving the road-side coil. When the on-board coil is fully above the road-side coil, the power transfer is only changing slowly with the coupling coefficient, which is influenced by both the longitudinal movement and the lateral position as determined by the accuracy of the path tracking.

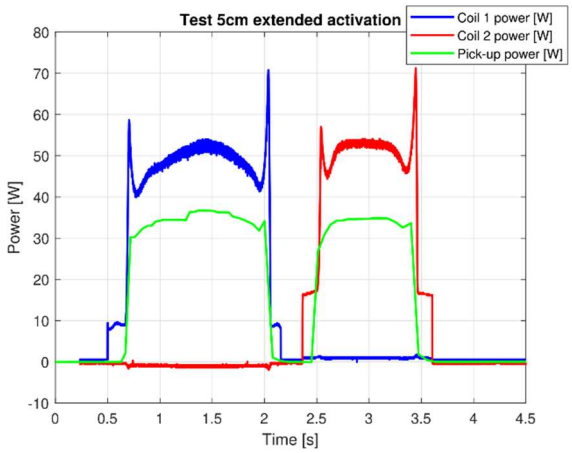

a) Activation 5 cm before the null-point

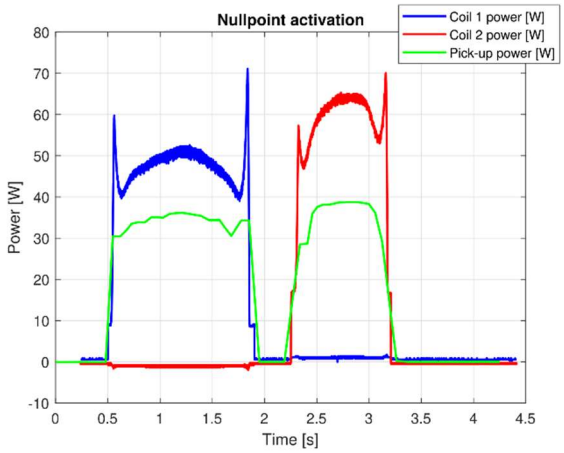

b) Activation at the null-point

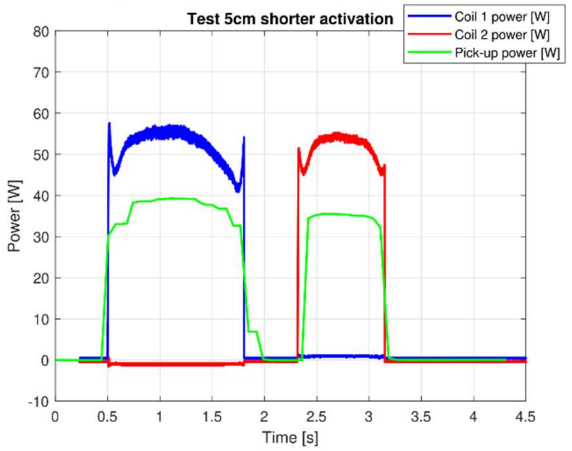

c) Activation 5 cm after passing the null-point

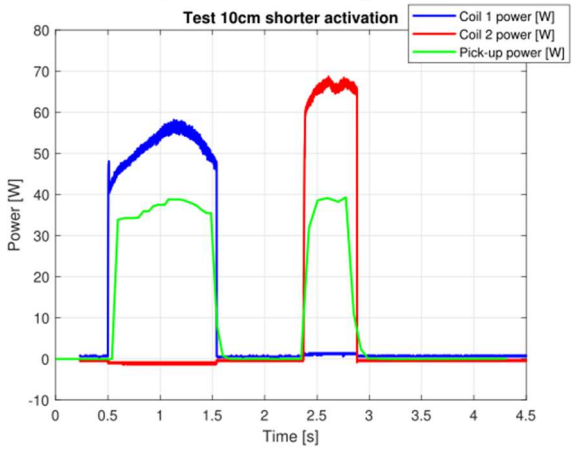

c) Activation 10 cm after passing the null-point

Fig. 12. Measured input and output power when road-side coils are activated at different positions of the truck model.

The curves in Fig. 11 clearly indicate that the instantaneous efficiency of the power transfer from the road-side infrastructure to the vehicle (i.e. $\eta(t) = P_{vehicle}(t)/P_{road}(t)$) changes significantly during one charging cycle. Thus, any instantaneous maximum or minimum value of the power transfer efficiency does not provide useful information about the utilization of the infrastructure. Instead, evaluation of the charging system performance should be based on the total energy, $E_{vehicle}$, transferred to the vehicle from one coil, and the corresponding energy transfer efficiency η_E [10]:

$$\eta_E = \frac{E_{vehicle}}{E_{road}} = \frac{\int_{t_{start}}^{t_{end}} P_{vehicle}(t)\,dt}{\int_{t_{start}}^{t_{end}} P_{road}(t)\,dt} \quad (1)$$

As given by (1), η_E is defined by the ratio between the input and output energy of the system during one charging cycle of a coil, lasting from the time t_{start} when the road-side coil is activated until t_{end} when the operation of the road-side coil is stopped.

In a second test condition, the road-side coils were activated at the point when the vehicle-side coil first reaches the road-side coil. Thus, the coil activation occurs 5 cm before reaching the null-point of the coupling. The results are shown in Fig. 12 a) which clearly shows that the idling period when losses are generated in the road-side coils without transferring power to the on-board coil is shorter than in Fig. 11. Since the power transfer is approximately the same as in the case from Fig. 11, with the only difference being due to minor variations in the path tracking, the energy transferred to the on-board battery is also approximately the same. Thus, the energy efficiency, η_E, is increased compared to the first case.

As a third test condition, the road-side coils were activated and deactivated at the null-points, which coincides with the point where the vehicle-side coil can start receiving power from the road-side coils. The results are presented in Fig. 12 b), which shows how this activation point allows the road-side coils to transfer power to the vehicle-side coil without any idling time before activation. Thus, this operation strategy would generally provide the same energy transfer capability as the previous cases but with lower total energy loss. However, there charging sequence still includes operation at very low coupling close to the null-points when entering and leaving the road-side coils. Therefore, the losses during the transient are still higher than when the on-board coil is above the middle of the road-side coil, and this case cannot provide the highest energy transfer efficiency.

The fourth experimental condition involved activating the road-side coils when the on-board coil has passed 5 cm beyond the null-point of the coupling, and the results are shown in Fig. 12 c). As the dimensions of the on-board coil is 10x10 cm, this case corresponds to activation when the onboard coil is fully above the road-side coil with the ends aligned. As can be found from the plot of the coupling coefficient in Fig. 11, this position is just before the position when maximum coupling between the coils is reached. In this condition, the power spikes in the road-side coils are significantly reduced, but not completely avoided. Furthermore, a small dip in the input power is still noticed when passing the point of maximum coupling. However, the power transferred to the on-board coil is almost constant, except for a slightly reduced power level close to the ends of the road-side coil. With this operation strategy, the total energy transferred to the on-board battery will be generally lower than for activation at the null-point, but the energy transfer efficiency, η_E, can be higher.

The fifth test involved activation of the road-side coils when the on-board coil has passed 10 cm beyond the null-point, and the results are shown in Fig. 12 d). In this case, the peaks in the input power to the road-side coil are fully avoided, and the coupling coefficient should be almost constant during the power transfer if the on-board coil would be perfectly centered on the road-side coil. However, any deviations in the lateral positioning of the truck will also influence the power transfer along the middle section of the coil. The impact from variations in the lateral positioning of the path tracking operation can also be noticed by comparing the power when the on-board coil is above the middle of the road-side coils for the different cases in Fig. 11 and Fig. 12.

To further assess the variations in the lateral position of the autonomous truck model and the impact on the power transfer, the logged input and output powers for 5 laps on the marked track are shown in Fig. 13. The results are obtained for the case when the road-side coils are activated when the on-board coil has passed 5 cm beyond the null-point of the coupling. As can be seen from the figure, the transients when the truck is entering and leaving the road-side coils are almost identical for the different laps. However, there is a noticeable variation in the input power to the road-side coils when passing the middle of the coil where the coupling at perfect lateral alignment would be almost constant. Thus, there is also a corresponding variation in the power transferred to the onboard battery. Since the power transfer in the region with high coupling is mainly limited by the voltage of the sending side converter, the small deviations from the ideal lateral position of the on-board coil are causing a small increase in the power transfer.

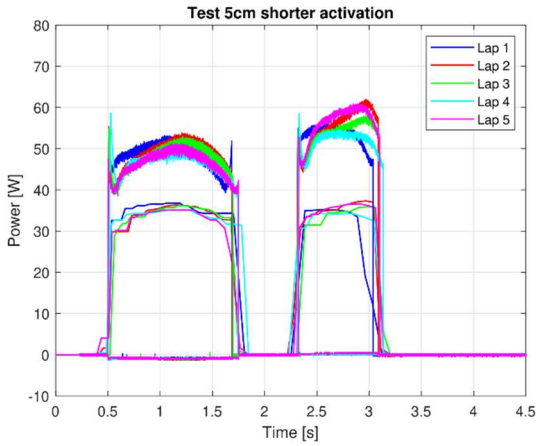

Fig. 13. Measured input and output power for 5 laps with activation 5 cm after the null-point of coupling

Table 2 Energy transfer and energy transfer efficiency with different strategies for activating the road-side coils.

Activation	Coil	Road-side energy [J]	Vehicle-side energy [J]	η_E
10 cm extended	1	76.24	45.64	0.60
	2	57.09	31.51	0.55
5 cm extended	1	71.53	46.41	0.65
	2	51.65	31.37	0.60
Null-point	1	65.46	44.49	0.68
	2	51.07	32.26	0.63
5 cm shorter	1	69.54	49.09	0.71
	2	41.03	25.43	0.62
10 cm shorter	1	53.74	33.80	0.63
	2	31.06	15.27	0.49

Thus, corresponding variations should be expected in the total energy transfer and energy transfer efficiency achieved with the two different the road-side coils sections.

The results for energy transfer and energy transfer efficiency from the cases presented in Fig. 11 and Fig. 12 are summarized in Table 1. The average of energy transfer efficiency for the two coils is also plotted in Fig. 14 to provide a visual image of the overall trend. The results in the table confirm how the energy transferred to the on-board battery do not change significantly when the road-side coils are activated around the null-point of the coupling. However, the energy efficiency is increased by delaying the activation of the road-side coils. Indeed, by delaying the activation of the road-side coils from 10 cm before the null-point to 5 cm before the null-point, the energy transfer efficiency is increased by 5 %. Delaying the activation until the null-point leads to another 2-3% of further increase of energy transfer efficiency.

If the activation of the road-side coil is delayed until the position of the on-board coil has passed the null-point with more than half the coil length, the received energy is significantly reduced. This is because energy is transferred also during the transient of the coupling, where the losses are higher than during the period when the receiving coil has high and almost constant coupling with the road-side coil. Thus, significant energy transfer potential is missed,

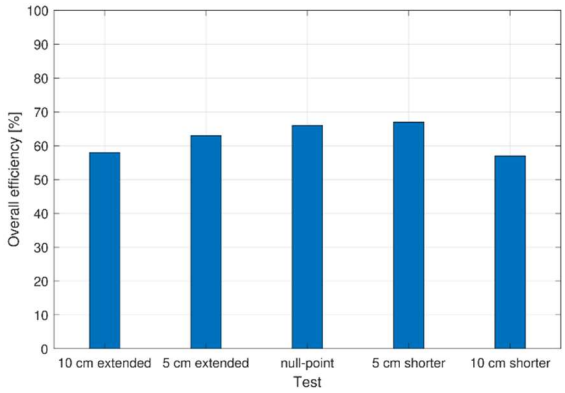

Fig. 14. Average energy transfer efficiency for the two coils with different activation points for the road-side coils.

and the energy transfer efficiency can even go down due to the turn-on and turn-off transients appearing in the period when the coupling and the power transfer capability is high.

It should be noted that the results in Table 1 and Fig. 14 are from a single run of the vehicle for each case. Thus, they are influenced by small variations in the lateral position due to variations in the path tracking accuracy while passing the coils, as illustrated in Fig. 13. However, the results illustrate the general trend as discussed for each of the cases in Fig. 12, and are in line with the results obtained with a rail-based setup in [10]. Furthermore, the results also indicate how the energy transfer efficiency is generally lower for the shortest coil. While part of this difference is due to a lower Q-factor, the shorter length also implies that the transients of entering and leaving the coil section influences a higher share of the total available time for power transfer.

CONCLUSION

This paper presents an evaluation of energy transfer efficiency of a dynamic wireless power transfer (DWPT) system utilized by a small-scale autonomous truck model. The truck models operates with a camera-vision-based path tracking on a track that includes two road-side coil sections for DWPT to the vehicle. The results demonstrate how it is important to assess the overall energy transfer efficiency of the system, and not the instantaneous power transfer efficiency, as the latter varies significantly while passing the road-side coil sections. Furthermore, it is shown that operating the system to transfer power during the transient phases when the vehicle is entering and leaving the road-side coils can maximize the energy transfer. However, the efficiency of the process is slightly reduced compared to operating the system only when the coupling between the coils is hight.

ACKNOWLEDGMENT

This work was supported by the Research Council of Norway (RCN) under Project number 304213, "Research and Demonstration of Key Technologies for Intelligent-connected Electric Vehicles in China and Norway" ("KeyTech NeVeChiNo).

REFERENCES

(1) S. Y. Choi, B. W. Gu, S. Y. Jeong, C. T. Rim, "Advances in Wireless Power Transfer Systems for Roadway-Powered Electric Vehicles," in *IEEE Journal of Emerging and Selected Topics in Power Electronics*, Vol. 3, No, 1, March 2015, pp. 18-36

(2) C. C. Mi, G. Buja, S. Y. Choi, C. T. Rim, "Modern Advances in Wireless Power Transfer Systems for Roadway Powered Vehicles," in IEEE Transactions on Industrial Electronics, Vol. 63, No. 10, October 2016, pp. 6533-6545

(3) EU FP7 Project, Fabric – Feasibility analysis and development of on-road charging solutions for future electric vehicles, http://www.fabric-project.eu/

(4) "Arena del Futuro - Innovative Dynamic Induction Charging Becomes a Reality https://www.stellantis.com/en/news/press-releases/2021/december/arena-del-futuro-innovative-dynamic-induction-charging-becomes-a-reality

(5) Smartroad Gotland project website, accessed November 2022: https://www.smartroadgotland.com/

(6) V. Skrickij, E. Šabanovič, V. Žuraulis, "Autonomous road vehicles: recent issues and expectations," in *IET Intelligent Transport Systems*, Vol. 14, No. 6, June 2020, pp. 471-479.

(7) M. Kane, "Wireless Charging And Autonomous Electric Cars Go Hand-In Hand", InsideEVs, https://insideevs.com/wireless-charging-autonomous-electric-cars/

(8) G. Guidi, A. M. Lekkas, J. E. Stranden, and J. A. Suul, "Dynamic wireless charging of autonomous vehicles: Small-scale demonstration of inductive power transfer as an enabling technology for self-sufficient energy supply," *IEEE Electrification Magazine*, vol. 8, no. 1, pp. 37–48, 2020.

(9) G. Guidi, "Small-scale model of inductive charging system for long-haul trucks," Project report, Available online from: https://www.sintef.no/globalassets/project/elingo/18-0733-rapport-8-memo-small-scale-model-til-nett.pdf.

(10) G. Guidi and J. A. Suul, "Transient control of dynamic inductive EV charging and impact on energy efficiency when passing a roadside coil section," in 2018 IEEE PELS Workshop on Emerging Technologies: Wireless Power Transfer (Wow). IEEE, 2018, pp. 1–7.

(11) G. Guidi, J. A. Suul, "Minimizing Converter Requirements of Inductive Power Transfer Systems with Constant Voltage Load and Variable Coupling Conditions," in *IEEE Transactions on Industrial Electronics*, Vol. 63, No. 11, November 2016, pp. 6835-6844

(12) G. Guidi, J. A. Suul, H. Fujimoto, "Conditions for maximum energy transfer in inductive road-powered electric vehicle applications taking system limitations into account," in *Proceedings of the* 5th International Electric Vehicle Technology Conference, EVTeC 2021, Yokohama, Japan / Virtual Conference, 24-26 May 2021, 8 pp.

(13) J. E. Stranden, "*Autonomous driving of a small-scale electric truck model with dynamic wireless charging*," MSc Thesis, Norwegian University of Science and Technology. (NTNU), June 2019

(14) A. Khalaf, "*Optimization of transfer efficiency of a dynamic wireless charging system for electric vehicles*," MSc Thesis, NTNU, June 2020

(15) M. Jørgensen, "*Computer vision based path tracking for a small-scale electric truck model with dynamic or static wireless charging*," MSc Thesis, NTNU, June 2021